

# Manifestation of the $P$ -wave diproton resonance in single-pion production in $pp$ collisions

M. N. Platonova\* and V. I. Kukulin†

*Skobeltsyn Institute of Nuclear Physics, Lomonosov Moscow State University, Moscow 119991, Russia*  
(Received 12 July 2016; published 27 September 2016)

It is demonstrated that many important features of single-pion production in  $pp$  collisions at intermediate energies ( $T_p \approx 400$ – $800$  MeV) can naturally be explained by supposing excitation of intermediate diproton resonances in  $pp$  channels  $^1D_2$ ,  $^3F_3$  and  $^3P_2$ , in addition to conventional mechanisms involving an intermediate  $\Delta$ -isobar. We predict for the first time the crucial role of the  $^3P_2$  diproton resonance, found in recent experiments on the single-pion production reaction  $pp \rightarrow pp(^1S_0)\pi^0$ , in reproducing the proper behavior of spin-correlation parameters in the reaction  $pp \rightarrow d\pi^+$  which were poorly described by conventional meson-exchange models to date. The possible quark structure of the  $P$ -wave diproton resonances is also discussed.

DOI: 10.1103/PhysRevD.94.054039

## I. INTRODUCTION: BRIEF HISTORICAL EXCURSUS

The activity in searching for dibaryon resonances in the 1980s was motivated by the success of MIT-bag models in the prediction of dibaryon states [1–3]. Numerous experiments on  $\vec{p}\vec{p}$  elastic scattering done at the same time revealed the possible existence of a series of diproton resonances with masses in the range 2.1–2.9 GeV and total widths 100–200 MeV [4–8]. Further studies established that these resonances are mainly of an inelastic nature and seen primarily in inelastic channels like  $pp \rightarrow d\pi^+$ ,  $pp \rightarrow pn\pi^+$ , etc. [9]. Using different data sets, a few groups performed partial-wave analyses (PWA) of  $pp$  and  $\pi^+d$  elastic scattering and the  $pp \leftrightarrow d\pi^+$  reaction [10–15] and found resonance poles in the  $^1D_2$ ,  $^3F_3$ ,  $^3P_2$ ,  $^1G_4$  and other  $NN$  channels. However some authors suggested the observed singularities to be related to the so-called pseudoresonances (see, e.g., [16]), which means rather generation of a resonance in a subsystem instead of the true diproton resonance in a whole interacting system. In the case of  $pp$  scattering at energies  $T_p \approx 600$  MeV, the pseudoresonance implies an intermediate  $\Delta$ -isobar generation coupled strongly to the rest nucleon. Thus, the resonance behavior of the  $pp$  elastic and inelastic scattering amplitudes is basically associated with the nearby  $N\Delta$  thresholds in the respective partial waves [17,18]. Similar discussions about dibaryon resonances near the  $\Delta\Delta$  threshold were very active for the last three decades, at least (see, e.g., [19]).

This rather indefinite situation began to change only in recent years when an experimental group using the  $4\pi$  detector WASA installed at the COSY facility (Juelich)

together with the SAID Data Analysis Center announced [20,21] the discovery of an  $I(J^P) = 0(3^+)$  dibaryon resonance  $d^*$  with a mass  $M_{d^*} \approx 2.38$  GeV in the  $^3D_3$ – $^3G_3$  channels of the  $NN$  system both in  $2\pi$ -production reactions and  $\vec{n}\vec{p}$  elastic scattering. This resonance, called an “inevitable dibaryon” [22], had been sought after for 50 years since its first prediction by Dyson and Xuong in 1964 [23]. Remarkably, the  $d^*$  dibaryon was predicted in [23] to belong to the same SU(3) multiplet as the deuteron—the lowest isoscalar dibaryon—while the  $^1D_2$  dibaryon was predicted to belong to the same SU(3) multiplet as the singlet deuteron—the lowest isovector dibaryon. Very recently another experimental group which uses the forward detector ANKE at the COSY facility has uncovered evidence [24] of the  $^3P_2$  and  $^3P_0$  diproton resonances with a mass  $M_D \approx 2.2$  GeV in the reaction  $pp \rightarrow (pp)_0\pi^0$ , where  $(pp)_0$  means the  $^1S_0$  singlet deuteron near-threshold state.

From the theoretical side, the calculations [25,26] within the framework of rigorous three-body  $\pi NN$  and  $\pi N\Delta$  models revealed; a robust  $^1D_2$  dibaryon resonance pole near the  $N\Delta$  threshold and also a  $^3D_3$  resonance pole near (below) the  $\Delta\Delta$  threshold. Furthermore, the recent quark model studies of the  $d^*$  dibaryon strongly support its unconventional nature as being a genuine six-quark state rather than just a  $\Delta$ – $\Delta$  bound state. Indeed, the observed width and decay properties of this resonance can be explained only if one assumes that it is dominated by a “hidden-color” six-quark configuration [27–29]. The hidden-color six-quark states are a rigorous first-principle prediction of SU(3) color gauge theory [30,31]. We also cite in this connection the recent issue of CERN Courier [32]: “COSY confirms existence of six-quark states.” So, in light of these new findings, one may hope that the long-term dispute between the supporters of the near-threshold singularities in  $N\Delta$  and  $\Delta\Delta$  channels and the apologists

\*platonova@nucl-th.sinp.msu.ru

†kukulin@nucl-th.sinp.msu.ru

of the true dibaryon resonances will shortly come to its completion.

To consider the dispute between the two alternatives above from the general physical point of view, we should say that as was recognized long ago by Baz [33], who developed Wigner's ideas [34] on the near-threshold cross section singularities in the field of nuclear reactions, there should be (in the majority of nuclei) a strong correlation between the position of a threshold for some channel  $B + C$  in a nucleus  $A = B + C$  and the near-threshold energy levels with appropriate quantum numbers. It is because the fragments  $B$  and  $C$  can move far apart near the channel threshold, keeping thereby their identity, so that a near-threshold bound (or resonance) state is very likely to emerge. A careful inspection [35] of the well-known nuclear level tables [36] actually confirmed the close correlation between the channel thresholds and the nearby bound states in many nuclei (e.g.,  $^{12}\text{C}^* \rightarrow ^8\text{Be} + \alpha$ ,  $^{16}\text{O}^* \rightarrow ^{12}\text{C}^* + \alpha$ , etc.). Hence, it can be supposed quite naturally that there is a strong correlation between thresholds and the nearby bound (or resonance) states also in hadronic physics [37,38]. A good example may be the Roper resonance  $N^*(1440)$ , its average pole mass<sup>1</sup> being  $M_{\text{pole}} \approx 1365$  MeV [40]. In fact, it has been found experimentally [41,42] that the very large (or even dominating) decay mode for the Roper resonance is the light scalar  $\sigma$ -meson emission (with  $m_\sigma \approx 400$ – $500$  MeV), so that the Roper can be treated as a near-threshold state in the  $\sigma + N$  channel [43]. The recent Faddeev calculations for “meson-assisted dibaryons” [44] seem to confirm the general correlation between thresholds and the nearby bound (or resonance) states in the dibaryon field as well.

Moreover, QCD does not forbid the existence of multi-quark states near thresholds or elsewhere. Recent experimental discoveries of the tetra- and pentaquarks [45,46] have confirmed the existence of exotic multi-quark states in general. So, in view of all these new achievements, studying the properties of multi-quark states and their manifestation in the basic hadronic processes has become of particular importance now.

The present paper is dedicated to the study of the manifestation of diproton (dibaryon) resonances in single-pion production in  $pp$  collisions in the GeV region. The main emphasis will be given to the basic pion-production reaction  $pp \rightarrow d\pi^+$  at energies  $T_p \approx 400$ – $800$  MeV where a few PWA as well as a rich set of experimental data exist. In [47] we elaborated on a model which combines two dominating conventional mechanisms of this reaction, i.e., one-nucleon exchange and an intermediate  $\Delta$  excitation, with the resonance mechanisms based on intermediate dibaryon excitation. By reexamining

the conventional  $\Delta$ -excitation mechanism, we have shown its strong sensibility to the short-range cutoff parameters  $\Lambda$  in meson-baryon vertices, especially in the  $\pi N\Delta$  vertex. Thus, when using “soft” cutoff parameters which naturally arise from the description of  $\pi N$  elastic scattering in the  $\Delta$  region, the conventional meson-exchange mechanisms give a strong underestimation for the partial and total  $pp \rightarrow d\pi^+$  cross sections. So, we have shown that the significant contribution should come from other sources (of the short-range nature), and that excitation of intermediate dibaryons in the dominant partial waves  $^1D_2P$  and  $^3F_3D$  of the reaction  $pp \rightarrow d\pi^+$  can really give this lacking contribution.

To our knowledge, the only attempt (besides the PWA) to describe the reaction  $pp \rightarrow d\pi^+$  at energies  $T_p \approx 400$ – $800$  MeV including dibaryon resonances was made previously in [48,49]. The authors used essentially the same model as we did in [47], but with a more sophisticated treatment of  $NN \rightarrow N\Delta$  amplitudes, and came to a conclusion similar to ours, that the conventional mechanisms give only half of the total cross section. Then, by fitting the parameters of six hypothetical dibaryon resonances to the existing experimental data, they also revealed the importance of two dibaryon resonances,  $^1D_2$  and  $^3F_3$ , in reproducing the total and differential cross sections and also the proton analyzing power. However, the masses of resonances other than  $^1D_2$  and  $^3F_3$  were found in their analysis to be too low, and their widths too narrow. Besides that, their model calculations could not reproduce the spin-correlation parameters properly. On the contrary, we fit the results of the most recent PWA [50,51] rather than experimental data, and include dibaryons only in three dominant partial waves,  $^1D_2P$ ,  $^3F_3D$  and (in the present paper)  $^3P_2D$ , where the resonance behavior of the amplitudes is well established. Thus, we can extract the dibaryon parameters more precisely and judge the role of individual resonances in  $pp \rightarrow d\pi^+$  observables.

In the present study, we focus on differential observables of the reaction  $pp \rightarrow d\pi^+$  and on the role of the  $P$ -wave diproton resonance which can be excited in the  $^3P_2D$  partial wave of the reaction. The  $^3P_2$  diproton resonance found previously in the PWA of  $pp$  elastic scattering [52,53] and confirmed in a recent experiment on the reaction  $pp \rightarrow (pp)_0\pi^0$  [24] has received much less attention in the literature than the  $^1D_2$  and  $^3F_3$  resonances. As we will show in the paper, the  $^3P_2$  dibaryon, though giving a small contribution ( $< 10\%$ ) to the total  $pp \rightarrow d\pi^+$  cross section, is very important for reproducing the differential observables, especially spin-correlation parameters, which have been poorly described by the conventional meson-exchange models to date [54–56] and also by a model [48,49] which included dibaryon resonances.

The structure of the paper is the following. In Sec. II the working model for treatment of the reaction  $pp \rightarrow d\pi^+$  with both intermediate  $\Delta$ 's and dibaryons is formulated. In

<sup>1</sup>One should bear in mind that a double-pole structure with two almost degenerate poles was found for the Roper resonance in [39] and recently confirmed by ANL-Osaka and Juelich groups.

Sec. III a description of the partial cross sections in the dominant partial waves  $^1D_2P$ ,  $^3F_3D$  and  $^3P_2D$  and also of the total cross section in a broad energy range is given. Section IV is devoted to discussion of the differential cross section, as well as vector analyzing powers and spin-correlation parameters, at energy  $T_p = 582$  MeV. In Sec. V the basic results attained in the paper are summarized and discussed.

## II. THEORETICAL MODEL

In this section, we briefly outline our model formalism for the reaction  $pp \rightarrow d\pi^+$ . The details can be found in Ref. [47]. The model includes three basic mechanisms depicted in Fig. 1. Two conventional mechanisms, i.e., one-nucleon exchange and excitation of the intermediate  $N\Delta$  system by the  $t$ -channel pion exchange, are shown in Figs. 1(a) and 1(b), respectively. Further on, we will refer to these mechanisms as ONE and  $N\Delta$ . An excitation of the intermediate  $\Delta$  isobar through the  $\rho$ -meson exchange has also often been considered in the literature [57], but such a mechanism contributes significantly only when choosing very high cutoff parameters in the meson-baryon form factors. Here, we choose the low values for the cutoff parameters  $\Lambda < 1$  GeV (reasons for this will be given below), for which the contribution of the  $\rho$ -exchange mechanism is very small.

In a standard approximation of the spectator nucleon [57], the helicity amplitudes corresponding to the mechanisms ONE and  $N\Delta$  take the form

$$\mathcal{M}_{\lambda_1, \lambda_2; \lambda_d}^{(\text{ONE})} = -\sqrt{2}(2m)^{3/2} \chi^\dagger(\lambda_2) i\sigma_2 \times \Psi_d^*(\boldsymbol{\rho}_a, \lambda_d) F_{\pi NN}(\eta_a) (\boldsymbol{\sigma}\boldsymbol{\eta}_a) \chi(\lambda_1), \quad (1)$$

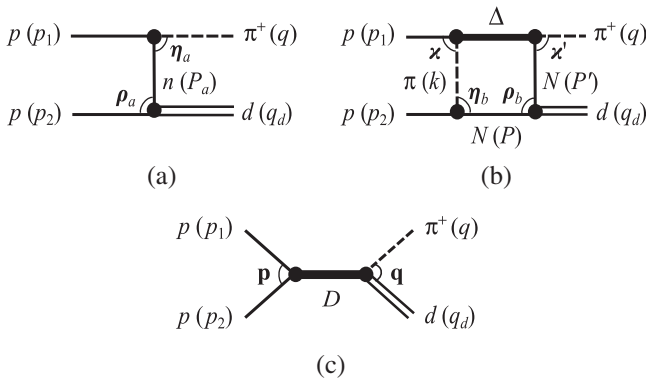


FIG. 1. Diagrams illustrating three basic mechanisms for the reaction  $pp \rightarrow d\pi^+$ : (a) one-nucleon exchange, (b) intermediate  $\Delta$ -isobar excitation, and (c) intermediate dibaryon resonance. The 4-momenta of the particles are shown in parentheses, and the 3-momenta in pair center-of-mass systems are denoted by boldface.

$$\begin{aligned} \mathcal{M}_{\lambda_1, \lambda_2; \lambda_d}^{(N\Delta)} &= -4\sqrt{2}/3(2m)^{1/2} \chi^\dagger(\lambda_2) i\sigma_2 \\ &\times \int \frac{d^3P}{(2\pi)^3} \frac{F_{\pi NN}(\eta_b) (\boldsymbol{\sigma}\boldsymbol{\eta}_b)}{w_\pi^2 - m_\pi^2 + i0} \\ &\times \Psi_d^*(\boldsymbol{\rho}_b, \lambda_d) \sqrt{\frac{\Gamma_\Delta(\boldsymbol{x}) \Gamma_\Delta(\boldsymbol{x}')}{\boldsymbol{x}^3 \boldsymbol{x}'^3}} \\ &\times \frac{16\pi W_\Delta^2 (\boldsymbol{x}\boldsymbol{x}' + i\frac{\boldsymbol{g}}{2} \boldsymbol{x} \times \boldsymbol{x}')}{W_\Delta^2 - M_\Delta^2 + iW_\Delta \Gamma_\Delta(W_\Delta)} \chi(\lambda_1), \end{aligned} \quad (2)$$

where  $w_\pi^2 = k^2$ , and the  $\Delta$ -isobar width is related to the vertex function  $F_{\pi N\Delta}$  as

$$\Gamma_\Delta(\boldsymbol{x}) = \frac{\boldsymbol{x}^3 m}{6\pi W_\Delta} F_{\pi N\Delta}^2(\boldsymbol{x}). \quad (3)$$

To calculate the spin structure of the amplitudes, it is convenient to write the deuteron wave function as

$$\Psi_d(\boldsymbol{\rho}, \lambda_d) = \boldsymbol{\sigma}\boldsymbol{\epsilon}(\boldsymbol{\rho}, \lambda_d), \quad (4)$$

where we have introduced the vector

$$\boldsymbol{\epsilon}(\boldsymbol{\rho}, \lambda_d) = u(\rho) \boldsymbol{\epsilon}(\lambda_d) + \frac{w(\rho)}{\sqrt{2}} \left( \boldsymbol{\epsilon}(\lambda_d) - \frac{3\rho(\boldsymbol{\rho}\boldsymbol{\epsilon}(\lambda_d))}{\rho^2} \right). \quad (5)$$

Here,  $\boldsymbol{\epsilon}(\lambda_d)$  is the standard deuteron polarization vector, and  $u$  and  $w$  are the  $S$ - and  $D$ -wave components of the deuteron wave function (DWF) normalized as  $\int d^3\rho (u^2 + w^2)/(2\pi)^3 = 1$ .

The helicity amplitudes antisymmetrized over two initial protons take the form

$$\mathcal{M}_{\lambda_1, \lambda_2; \lambda_d}^{(s)}(\theta) = \mathcal{M}_{\lambda_1, \lambda_2; \lambda_d}(\theta) + (-1)^{\lambda_d} \mathcal{M}_{\lambda_2, \lambda_1; \lambda_d}(\pi - \theta). \quad (6)$$

Overall, there are six independent helicity amplitudes in the reaction  $pp \rightarrow d\pi^+$  [56]:

$$\begin{aligned} \Phi_1 &= \mathcal{M}_{\frac{1}{2}, \frac{1}{2}; 1}^{(s)}, & \Phi_2 &= \mathcal{M}_{\frac{1}{2}, \frac{1}{2}; 0}^{(s)}, & \Phi_3 &= \mathcal{M}_{\frac{1}{2}, \frac{1}{2}; -1}^{(s)}, \\ \Phi_4 &= \mathcal{M}_{\frac{1}{2}, -\frac{1}{2}; 1}^{(s)}, & \Phi_5 &= \mathcal{M}_{\frac{1}{2}, -\frac{1}{2}; 0}^{(s)}, & \Phi_6 &= \mathcal{M}_{\frac{1}{2}, -\frac{1}{2}; -1}^{(s)}. \end{aligned} \quad (7)$$

For comparison of the theoretical results with the PWA data and for studying the contributions of the intermediate dibaryon resonances, it is convenient to deal with the partial-wave amplitudes, which are expressed through the helicity ones via the standard formulas given by Jacob and Wick [58]. The dominant partial-wave amplitudes in a broad energy range including the region of  $\Delta$  excitation, as was shown by  $\pi^+d \rightarrow pp$  PWA [see, e.g., Fig. 5(b) in Ref. [50]], are  $^1D_2P$ ,  $^3F_3D$  and  $^3P_2D$  (with decreasing magnitude). The explicit formulas for these amplitudes are

$$A(^1D_2P) = \frac{1}{2}\sqrt{\frac{3}{5}}(\Phi_1^{(2)} + \Phi_3^{(2)}) + \frac{1}{\sqrt{5}}\Phi_2^{(2)}, \quad (8)$$

$$A(^3F_3D) = -\frac{2}{\sqrt{7}}\Phi_4^{(3)} - \frac{1}{2}\sqrt{\frac{6}{7}}\Phi_5^{(3)}, \quad (9)$$

$$A(^3P_2D) = \sqrt{\frac{1}{10}}(\Phi_1^{(2)} - \Phi_3^{(2)}) + \sqrt{\frac{3}{5}}\Phi_4^{(2)}, \quad (10)$$

where

$$\Phi_i^{(J)} = \int_{-1}^1 d_{\lambda_1-\lambda_2,-\lambda_d}^{(J)}(x)\Phi_i(x)dx, \quad x = \cos(\theta). \quad (11)$$

For the amplitude corresponding to excitation of an intermediate dibaryon resonance [see Fig. 1(c)], it is convenient to start from the partial-wave representation. The respective amplitude is

$$A^{(D)}(^{2S+1}L_JL_\pi) = -\frac{8\pi s}{\sqrt{pq}s - M_D^2 + i\sqrt{s}\Gamma_D(s)}, \quad (12)$$

where  $p = (s - 4m^2)^{1/2}/2$  and  $q = [(s - m_\pi^2 - m_d^2)^2 - 4m_\pi^2 m_d^2]^{1/2}/2\sqrt{s}$  are the moduli of the proton and the pion c.m. system momenta, respectively. The factor 2 before the incoming width  $\Gamma_i(s)$  was introduced to account for two identical protons in the initial state.

For the incoming width  $\Gamma_i(s) \equiv \Gamma_{D \rightarrow pp}(s)$ , we used the Gaussian parametrization which follows from the  $D \rightarrow NN$  form factor parametrization employed in the dibaryon model for the  $NN$  interaction [59,60]:

$$\Gamma_i(s) = \Gamma_i\left(\frac{p}{p_0}\right)^{2L+1} \exp\left(-\frac{p^2 - p_0^2}{\alpha_{pp}^2}\right), \quad (13)$$

where  $p_0$  is the value of the  $pp$  relative momentum at  $\sqrt{s} = M_D$ .

For the outgoing width  $\Gamma_f(s) \equiv \Gamma_{D \rightarrow \pi^+ d}(s)$ , we employed the parametrization analogous to that for the  $\Delta \rightarrow \pi N$  width [cf. (3) with a monopole form factor (25)]:

$$\Gamma_f(s) = \Gamma_f\left(\frac{q}{q_0}\right)^{2L_\pi+1} \left(\frac{p_0^2 - \Lambda_{\pi d}^2}{p^2 - \Lambda_{\pi d}^2}\right)^{L_\pi+1}, \quad (14)$$

where  $q_0$  is the value of the  $\pi d$  relative momentum at  $\sqrt{s} = M_D$ . This parametrization was proposed for  $\pi N$  and  $KN$  elastic scattering in [61,62] and then applied for the  $\pi^+ d \rightarrow pp$  PWA in [13]. The same energy dependence was assumed here also for the total dibaryon width  $\Gamma_D(s)$ , since, due to the high inelasticity of dibaryon resonances, the incoming width  $\Gamma_{D \rightarrow pp}$  is only a small fraction ( $\sim 10\%$ ) of the total width [18].

By using Eq. (12) and the Jacob-Wick formulas [58] which are an inversion of Eqs. (8)–(10), one can find the

contributions from intermediate dibaryons to the helicity amplitudes  $\Phi_i$  ( $i = 1, \dots, 6$ ). One should also note that  $\Phi_6^{(J)} = \Phi_4^{(J)}$  for odd  $J$  and  $\Phi_6^{(J)} = -\Phi_4^{(J)}$  for even  $J$  [56]. Then the respective helicity amplitudes, when three dibaryon resonances are taken into account, take the form

$$\Phi_1^{(D)} = \left(\frac{\sqrt{15}}{2}A^{(D)}(^1D_2P) + \sqrt{\frac{5}{2}}A^{(D)}(^3P_2D)\right)d_{0,-1}^{(2)}(x),$$

$$\Phi_2^{(D)} = \sqrt{5}A^{(D)}(^1D_2P)d_{0,0}^{(2)}(x),$$

$$\Phi_3^{(D)} = \left(\frac{\sqrt{15}}{2}A^{(D)}(^1D_2P) - \sqrt{\frac{5}{2}}A^{(D)}(^3P_2D)\right)d_{0,1}^{(2)}(x),$$

$$\Phi_4^{(D)} = -\sqrt{7}A^{(D)}(^3F_3D)d_{1,-1}^{(3)}(x) + \frac{\sqrt{15}}{2}A^{(D)}(^3P_2D)d_{1,-1}^{(2)}(x),$$

$$\Phi_5^{(D)} = -\sqrt{\frac{21}{2}}A^{(D)}(^3F_3D)d_{1,0}^{(3)}(x),$$

$$\Phi_6^{(D)} = -\sqrt{7}A^{(D)}(^3F_3D)d_{1,1}^{(3)}(x) - \frac{\sqrt{15}}{2}A^{(D)}(^3P_2D)d_{1,1}^{(2)}(x). \quad (15)$$

One can see that the  $^1D_2P$  amplitude gives the dominant contribution to the helicity amplitudes  $\Phi_1$ – $\Phi_3$ , while the  $^3F_3D$  amplitude gives the dominant contribution to  $\Phi_4$ – $\Phi_6$ . At the same time, the  $^3P_2D$  amplitude introduces corrections to both sets of helicity amplitudes. As will be shown in Sec. IV, these corrections, though being rather small in magnitude, turn out to be crucial for polarization observables in the  $pp \rightarrow d\pi^+$  reaction.

The partial cross sections are expressed through the partial-wave amplitudes as follows:

$$\sigma(^{2S+1}L_JL_\pi) = \frac{(2J+1)q}{64\pi s} \frac{1}{p} |A(^{2S+1}L_JL_\pi)|^2. \quad (16)$$

Further, we give the expressions for observables in terms of six helicity amplitudes  $\Phi_i$  ( $i = 1, \dots, 6$ ), using the notations of Ref. [56] (apart from a  $2m$  factor in the amplitudes' normalization), with the signs of the polarization observables given in the Madison convention. A different notation for amplitudes and observables can be found in, e.g., [50].

For the total cross section, one has

$$\sigma(pp \rightarrow d\pi^+) = \frac{1}{64\pi s} \frac{q}{p} \int_{-1}^1 \sum_{i=1}^6 |\Phi_i(x)|^2 dx. \quad (17)$$

The following expressions hold for the differential cross section,

$$\frac{d\sigma}{d\Omega}(pp \rightarrow d\pi^+) = \frac{1}{64\pi^2 s} \frac{q}{p} \frac{1}{4} \Sigma, \quad (18)$$

$$\Sigma = 2 \sum_{i=1}^6 |\Phi_i|^2,$$

for proton and deuteron vector analyzing powers,

$$A_{y0} = 4\text{Im}(\Phi_1^*\Phi_6 + \Phi_3^*\Phi_4 - \Phi_2^*\Phi_5)\Sigma^{-1}, \quad (19)$$

$$iT_{11} = -\sqrt{6}\text{Im}[(\Phi_1^* - \Phi_3^*)\Phi_2 + (\Phi_4^* - \Phi_6^*)\Phi_5]\Sigma^{-1}, \quad (20)$$

and for proton-proton spin-correlation parameters,

$$A_{xx} = [4\text{Re}(\Phi_1^*\Phi_3 - \Phi_4^*\Phi_6) + 2|\Phi_5|^2 - 2|\Phi_2|^2]\Sigma^{-1}, \quad (21)$$

$$A_{yy} = [4\text{Re}(\Phi_1^*\Phi_3 + \Phi_4^*\Phi_6) - 2|\Phi_5|^2 - 2|\Phi_2|^2]\Sigma^{-1}, \quad (22)$$

$$A_{zz} = -2(|\Phi_1|^2 + |\Phi_2|^2 + |\Phi_3|^2 - |\Phi_4|^2 - |\Phi_5|^2 - |\Phi_6|^2)\Sigma^{-1}, \quad (23)$$

$$A_{xz} = 4\text{Re}(\Phi_1^*\Phi_6 + \Phi_3^*\Phi_4 - \Phi_2^*\Phi_5)\Sigma^{-1}. \quad (24)$$

There are also deuteron tensor analyzing powers and spin-correlation parameters for the proton and deuteron and for two protons and a deuteron [50,56]. However, experimental data exist for the above-defined observables only, so, in the present paper, we restrict our calculations to these observables.

The meson-baryon vertex functions  $F_{\pi NN}$  and  $F_{\pi N\Delta}$  were parametrized in a monopole form<sup>2</sup>

$$F_{\pi NN}(p, \tilde{\Lambda}) = \frac{f}{m_\pi} \frac{p_0^2 + \tilde{\Lambda}^2}{p^2 + \tilde{\Lambda}^2},$$

$$F_{\pi N\Delta}(p, \tilde{\Lambda}_*) = \frac{f_*}{m_\pi} \frac{p_0^2 + \tilde{\Lambda}_*^2}{p^2 + \tilde{\Lambda}_*^2}, \quad (25)$$

where  $p^2$  is the modulo squared of the  $\pi-N$  relative momentum (i.e., the pion momentum in the  $\pi N$  c.m. system) and  $p_0^2$  corresponds to the situation when all three particles are real, i.e., located on their mass shells (so,  $p_0^2$  is positive for  $\pi N\Delta$  and negative for the  $\pi NN$  vertex). The coupling constants in Eq. (25) have been taken to be  $f = 0.97$  and  $f_* = 2.17$ . In this case, one has  $f^2/4\pi = 0.075$ , and the above value for  $f_*$  was derived from the total width of the  $\Delta$  isobar  $\Gamma_\Delta = 117$  MeV as given by the Particle Data Group [40].

<sup>2</sup>The cutoff parameters  $\tilde{\Lambda}$  and  $\tilde{\Lambda}_*$  in Eq. (25) were marked by a tilde sign to distinguish them from parameters used in a more familiar monopole vertex parametrization which follows from Eq. (25) when only the pion is off shell (see Ref. [47] for details).

As was argued in [47], the main advantage of the above vertex parametrization is that it admits a straightforward off-shell continuation and describes the real and virtual particles *in a unified manner*. It does not require introducing any additional parameters to account for the particles leaving their mass shells. Hence, it can be used for consistent description of processes involving on- and off-shell pions, i.e.,  $\pi N \rightarrow \pi N$ ,  $NN \rightarrow \pi d$ , elastic  $NN$  scattering, etc., with the same cutoff parameters in meson-baryon vertices. Moreover, the cutoff parameters  $\tilde{\Lambda}$  in such a case do not need to be fitted *ad hoc* and can in general be found directly from experimental data.

Thus, the parameter  $\tilde{\Lambda}_*$  in the  $\pi N\Delta$  vertex can be found from empirical data on  $\pi N$  elastic scattering. From fitting the PWA (SAID) data [63] for the  $\pi N$ -scattering  $P_{33}$  partial cross section in a broad energy range within the isobar model, we found  $\tilde{\Lambda}_* = 0.3$  GeV (see Fig. 2). For the  $\pi NN$  vertex, we have chosen the value  $\tilde{\Lambda} = 0.7$  GeV, which was used in a number of previous calculations of single-pion production reactions [56,64]. This value of  $\tilde{\Lambda}$  is also consistent with the predictions of the lattice-QCD calculations [65,66].

A detailed discussion on the choice of short-range cutoff parameters and their strong impact on cross sections of the  $pp \rightarrow d\pi^+$  reaction can be found in our previous work [47]. It should be stressed here that the cutoff values chosen in our calculations are much lower than those traditionally used in the realistic  $NN$ -potential models. For example, in the Bonn model [67], the minimal values, which still allow a good description of  $NN$ -scattering phase shifts up to  $T_N = 350$  MeV, are  $\Lambda \approx \Lambda_* \approx 1.3$  GeV (in the CD-Bonn model [68] they are even higher). Such very high cutoff parameters apparently lead to increased meson-exchange contributions at

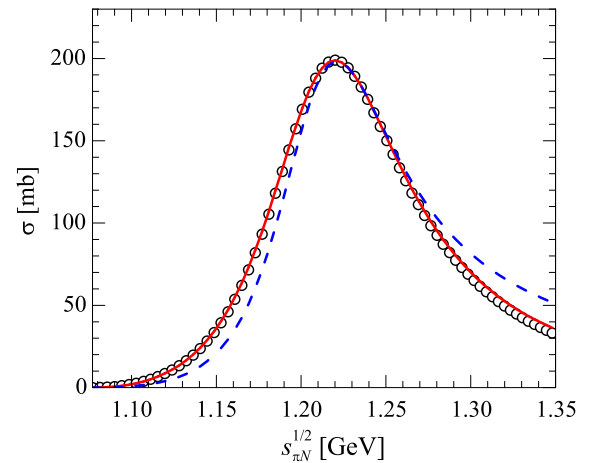


FIG. 2. The cross section of  $\pi N$  elastic scattering in the  $P_{33}$  partial wave. Solid and dashed lines show the calculations in the isobar model with the  $\pi N\Delta$  vertex in the form (25) and cutoff parameters  $\tilde{\Lambda}_* = 0.3$  and  $0.52$  GeV, respectively. Open circles correspond to the PWA data (SAID, solution WI08 [63]).

short internucleon distances. On the other hand, results of the numerous quark-model calculations agree, in general, that the parameters in meson-baryon vertices should be essentially soft, i.e.,  $\Lambda < 1$  GeV (see, e.g., [69] and references therein). In this case, one should seek for some alternative short-range mechanisms (such as formation of intermediate dibaryons) to describe the processes involving high momentum transfers within the two-nucleon system.

### III. RESULTS FOR THE PARTIAL AND TOTAL CROSS SECTIONS

Here we calculated partial and total cross sections for the reaction  $pp \rightarrow d\pi^+$  in the energy range  $\sqrt{s} = 2.03\text{--}2.27$  GeV ( $T_p \approx 320\text{--}860$  MeV) using the above formalism. Three dibaryon resonances generated in  $pp$  channels  $^1D_2$ ,  $^3F_3$  and  $^3P_2$  were included in the calculations. At the present stage, we restricted ourselves to an accurate description of the three dominant partial-wave amplitudes and to qualitative estimation of the dibaryon contributions in these amplitudes. We did not consider the possible dibaryons in small amplitudes (such as  $^1G_4$ ,  $^3P_1$ ,  $^1S_0$ , etc.), since the amount of evidence for these dibaryons is less to date than for the  $^1D_2$ ,  $^3F_3$  and  $^3P_2$  ones, and also description of the small amplitudes would require a more precise treatment of the background meson-exchange processes. Besides that, increasing the number of dibaryons would increase the number of model parameters and thus complicate making reliable conclusions.

For the consistency of our model, in calculations of conventional mechanisms ONE and  $N\Delta$ , we used the DWF derived in the dibaryon model for  $NN$  interaction [59,60]. This DWF has been truncated in the present study at high internucleon momenta  $p > 350$  MeV (with keeping the overall normalization) to prevent an unphysical rise of the differential cross section at large angles. So, the results obtained here with this regularized DWF turned out to be very close to those with the conventional CD-Bonn DWF [68].

Our model calculations were compared to the results of the most recent PWA (SAID, solution C500 [51,63]), which is a coupled-channel analysis using  $\pi^+d \rightarrow pp$ ,  $pp \rightarrow pp$  and  $\pi^+d \rightarrow \pi^+d$  experimental data. The dibaryon parameters obtained by fitting the partial cross sections in three dominant partial waves  $^1D_2P$ ,  $^3F_3D$  and  $^3P_2D$  to the PWA results are summarized in Table I. The relative phases  $\varphi$  between the resonance (dibaryon) and “background” (ONE +  $N\Delta$ ) amplitudes were fixed as shown in the last column of the table (these values coincide with the best-fit results up to several degrees).

The dibaryon masses and widths obtained in our fit are generally consistent with the previous estimates [10,70,71]. It is particularly important that the parameters of the  $^3P_2$  resonance found here are in very good agreement with those found in a recent experimental work [24] from a global fit of

TABLE I. Parameters of dibaryon resonances used in calculations of the reaction  $pp \rightarrow d\pi^+$ . In the last column, the phases  $\varphi$  of the dibaryon production amplitudes with respect to the “background” (ONE +  $N\Delta$ ) amplitude are shown.

$2S+1L_J$	$M_D$ (MeV)	$\Gamma_D$ (MeV)	$\Gamma_i\Gamma_f$ (MeV <sup>2</sup> )	$\alpha_{pp}$ (GeV)	$\Lambda_{\pi d}$ (GeV)	$\varphi$ (deg)
$^1D_2$	2155	101	74	0.23	0.27	0
$^3F_3$	2197	152	53	0.32	0.53	0
$^3P_2$	2211	195	450	3.0	0.26	180

experimental data on the differential cross section and proton analyzing power in the reaction  $pp \rightarrow (pp)_0\pi^0$ , i.e.,  $M_D = 2207 \pm 12$  and  $\Gamma_D = 170 \pm 32$  MeV.

Nevertheless, in determining these parameters, one should bear in mind the possible uncertainties associated with our model assumptions as well as with different PWA results. Thus, two SAID PWA solutions, i.e., the coupled-channel solution C500 [51,63] and the previous solution SP96 [63] for the  $\pi^+d \rightarrow pp$  reaction, give almost the same results for two dominating partial-wave amplitudes, but rather different results for the smaller  $^3P_2D$  amplitude at energies  $\sqrt{s} > 2.17$  GeV—see Fig. 3. Our present fit for the latter amplitude gives some average result between these PWA solutions. Further, in view of a large width of the  $^3P_2$  resonance, the extracted values of its parameters depend on the width parametrization used in the theoretical model. Thus, assuming the total width to be constant, we obtained for this resonance  $M_D = 2162$  and  $\Gamma_D = 154$  MeV. These values almost coincide with those found in [52] in the PWA of  $pp$  elastic scattering.

The results for the partial cross sections in three dominant partial waves are shown in the left panel of Fig. 3. The Argand plots for the respective amplitudes<sup>3</sup> are given in the right panel of Fig. 3.

As is seen from Fig. 3, the conventional mechanisms give approximately 40%–50% of the cross sections in the partial waves  $^1D_2P$  and  $^3F_3D$ . One should note that the initial- and final-state distortions, which are not included in our model, would further decrease the calculated cross sections by about 20% [56]. On the other hand, the  $N\Delta$  attraction generated by pion exchange can enhance the cross sections somehow [72]. We argue that this  $t$ -channel attraction which is governed by the cutoff parameters in the meson-baryon vertices should be very moderate when using soft cutoff values, and the basic short-range attraction in the  $N\Delta$  system would be induced in this case by generation of intermediate dibaryon resonances, similar to that found for the  $NN$  system in the dibaryon model for  $NN$  interaction [59,60]. Nevertheless, to examine possible

<sup>3</sup>Note that due to a different normalization, partial-wave amplitudes defined in Sec. II should be multiplied by a factor  $\sqrt{pq/s}/8\pi$  to be compared with the ones used in the SAID PWA [51].

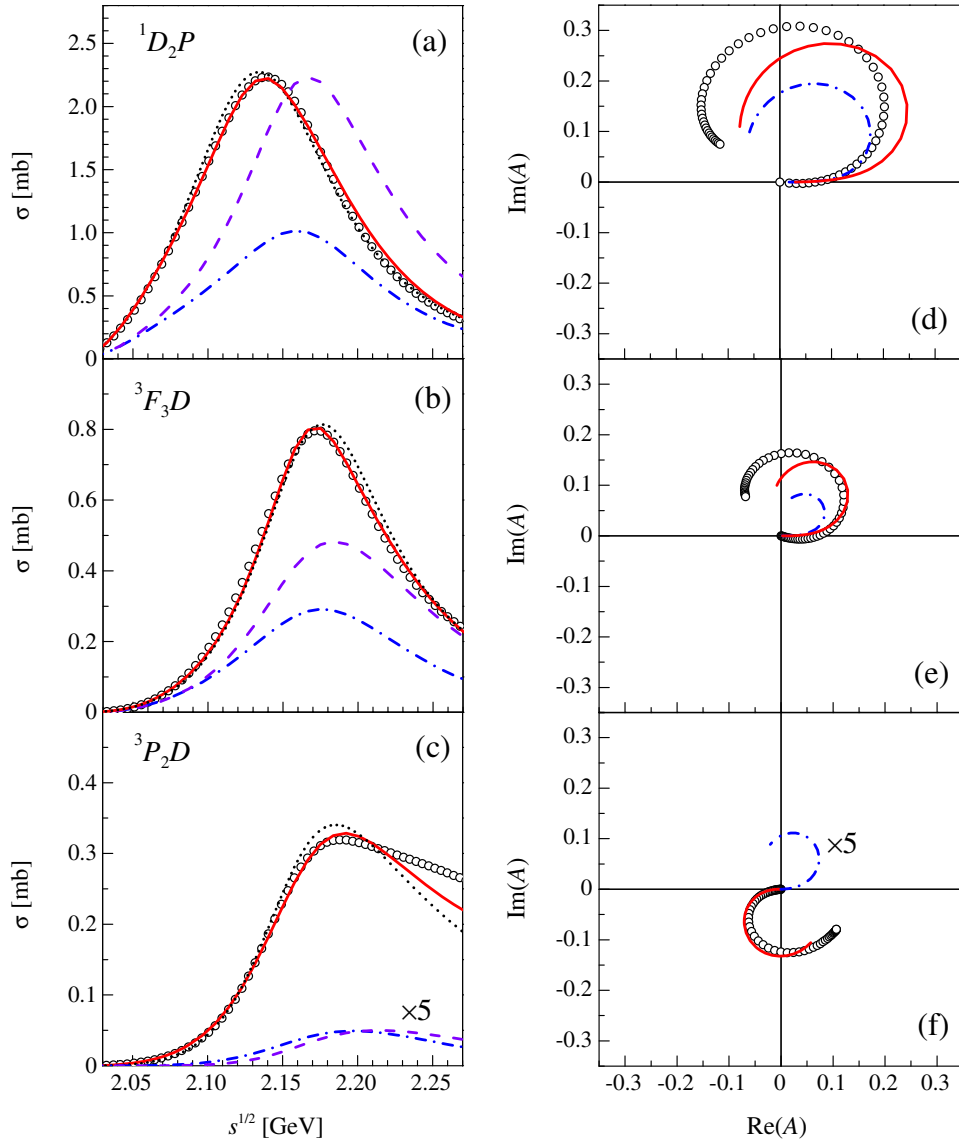


FIG. 3. Left panel: Partial cross sections of the reaction  $pp \rightarrow d\pi^+$  in the dominant partial waves (a)  $^1D_2P$ , (b)  $^3F_3D$  and (c)  $^3P_2D$ . Right panel: Argand plots for the dominant partial-wave amplitudes (d)  $^1D_2P$ , (e)  $^3F_3D$  and (f)  $^3P_2D$ . Dotted-dashed lines show the summed contributions of two conventional mechanisms ONE +  $N\Delta$  with a cutoff parameter  $\tilde{\Lambda}_* = 0.3$  GeV consistent with  $\pi N$  elastic scattering (see Fig. 2). The contributions of ONE+ $N\Delta$  mechanisms with an enhanced parameter  $\tilde{\Lambda}_* = 0.52$  GeV are shown by dashed lines. The ONE +  $N\Delta$  contributions in the  $^3P_2D$  channel were multiplied by a factor of 5 for better visibility. Results of the full model calculations including also intermediate dibaryon resonances are shown by solid lines. The open circles and dotted lines correspond to the PWA results (SAID, solutions C500 and SP96, respectively [51,63]).

effects of the  $N\Delta$   $t$ -channel interaction on the  $pp \rightarrow d\pi^+$  cross sections, one could strengthen the intermediate  $\Delta$  contribution through enhancing the cutoff parameter  $\tilde{\Lambda}_*$  in the  $\pi N\Delta$  vertex *ad hoc*. Thus, when enhancing  $\tilde{\Lambda}_*$  from 0.3 to 0.52 GeV, one is able to reproduce the magnitude of the  $^1D_2P$  partial cross section [see Fig. 3(a)]. Note, however, that this worsens simultaneously the description of  $P_{33}$   $\pi N$  elastic scattering (cf. Fig. 2). Further, as is shown in Fig. 3(b), the same cutoff parameter modification can also improve the description of the  $^3F_3D$  partial cross section, though not enough to reproduce its empirical behavior.

On the other hand, in the  $^3P_2D$  channel, the ONE +  $N\Delta$  mechanisms give only  $\sim 2.5\%$  of the partial cross section near the resonance peak, and this result very weakly depends on the  $\pi N\Delta$  cutoff parameter value [see Fig. 3(c)]. Thus, the intermediate  $\Delta$  excitation appears to play only a minor role in this channel. Besides that, the  $N\Delta$  amplitude has an improper phase here [see Fig. 3(f)]. So, a satisfactory description of the empirical data on the  $^3P_2D$  partial cross section cannot be attained through any changes in parameters of the conventional mechanisms, and an additional resonance contribution appears to be urgently needed. The

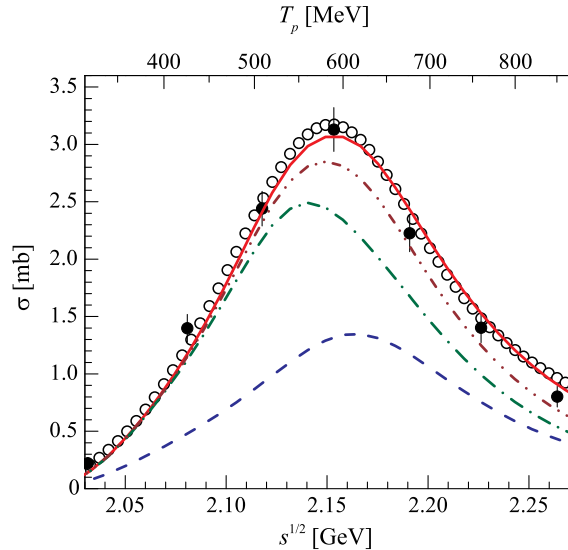


FIG. 4. Total cross section of the reaction  $pp \rightarrow d\pi^+$ . Dashed lines show the summed contributions of two conventional mechanisms ONE +  $N\Delta$ . Dotted-dashed, dash-dot-dotted and solid lines correspond to the results of model calculations including also one ( $^1D_2$ ), two ( $^1D_2 + ^3F_3$ ) and three ( $^1D_2 + ^3F_3 + ^3P_2$ ) intermediate dibaryon resonances, respectively. Open circles correspond to PWA results (SAID, solution C500 [51,63]) and filled circles to the experimental data [73].

crucial role of proper description of the  $^3P_2D$  partial-wave amplitude is particularly seen in the spin-correlation parameters, which will be discussed in the next section.

Here, we present also the results for the total cross section shown in Fig. 4. Though the conventional mechanisms reproduce a correct shape for the total cross section, the experimental data are underestimated by a factor of two, similar to the partial cross sections in two dominant partial waves. Taking the intermediate dibaryons into account fills in the discrepancy between the conventional-model calculations and the data, thus leading to very good reproduction of experimental data in the whole energy range considered.

#### IV. RESULTS FOR DIFFERENTIAL CROSS SECTION AND POLARIZATION OBSERVABLES AT $T_p = 582$ MEV

In this section, the results for differential observables in the reaction  $pp \rightarrow d\pi^+$  at energy  $T_p = 582$  MeV ( $\sqrt{s} = 2.15$  GeV) are presented. The energy value chosen here is close to that, where the total cross section has its maximum. Besides that, a rich set of experimental data exists in this energy region [74–78].

The results for the differential cross section are shown in Fig. 5. The differential cross section is described very well, except for the forward region, where high partial waves (giving a contribution less than 3% to the total cross section) obviously play an important role. Thus, one can see some underestimation of the contributions of these high partial

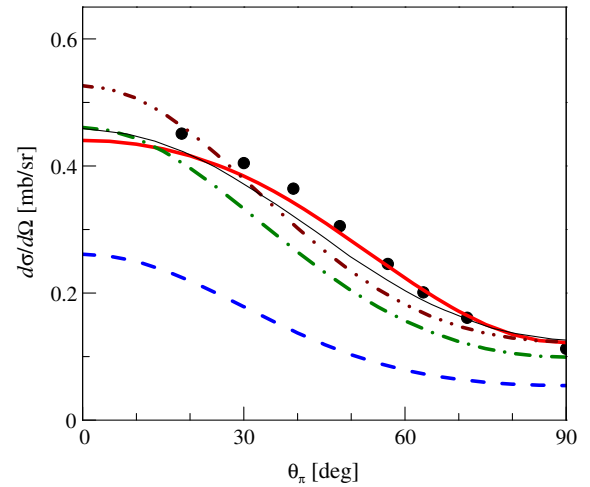


FIG. 5. Differential cross section in the reaction  $pp \rightarrow d\pi^+$  at energy  $T_p = 582$  MeV ( $\sqrt{s} = 2.15$  GeV). The meaning of theoretical curves is the same as in Fig. 4. The thin solid line corresponds to the conventional model calculations [54] including off-shell modifications and heavy-meson exchanges. Filled circles show the experimental data [74].

waves in our model. Further, the main contribution after the  $^3P_2D$  channel comes from  $S$ -wave pion production in the  $^3P_1S$  partial wave [50]. The  $S$ -wave pion production, which is important near the threshold, is usually described by some additional mechanism based on the phenomenological Lagrangian approach [57]. Some contribution to this term comes also from  $S$ -wave  $\pi N$  scattering in the intermediate state. Neither of these mechanisms are included in the present model. This is also the possible reason for a discrepancy between our calculation and experimental data for the proton analyzing power  $A_{y0}$  shown in Fig. 6(a). This observable is very sensitive to the small amplitudes in the nondominant partial waves, and especially, to the  $^3P_1S$  amplitude. In fact, just a few models were able to reproduce the shape of  $A_{y0}$  (see, e.g., [55,56]). It is so sensitive to the tiny details of the model that even the most accurate to date theoretical calculation based on solving exact Faddeev-type equations for the coupled  $\pi NN \leftrightarrow NN$  system [54] could not reproduce its proper behavior. In particular, as was shown in [79], inclusion of the small  $S$ - and  $P$ -wave  $\pi N$ -scattering amplitudes just in first order leads to a proper description of the “double-hump” shape of  $A_{y0}$ , but the exact inclusion of these small amplitudes gives again an improper behavior like that shown in Fig. 6(a). So, even the qualitative description of  $A_{y0}$  requires an extremely accurate theoretical treatment of small partial-wave amplitudes.

We also calculated the deuteron vector analyzing power  $iT_{11}$  [see Fig. 6(b)]. Its qualitative behavior is described properly already by conventional mechanisms, however, with a significant overestimation. Inclusion of dibaryon resonances, especially the  $^3P_2$  one, allows us to reduce the discrepancy with experimental data.

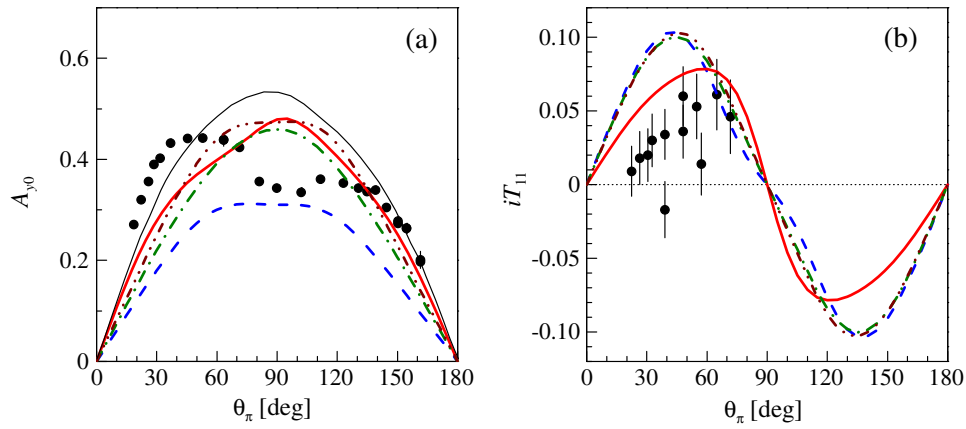


FIG. 6. (a) Proton and (b) deuteron vector analyzing powers in the reaction  $pp \rightarrow d\pi^+$  at energy  $T_p = 582$  MeV ( $\sqrt{s} = 2.15$  GeV). The meaning of theoretical curves is the same as in Fig. 5. Filled circles show the experimental data (a) [75] and (b) [76]. (The  $iT_{11}$  data [76] were obtained in an inverse process  $\pi^+d \rightarrow pp$  at  $T_\pi = 140$  MeV, corresponding to  $T_p = 562$  MeV.)

In general, one can conclude that our approximate model for conventional meson-exchange processes describes the experimental data for the basic observables not worse than more sophisticated theoretical models elaborated in previous years. The main difference is that we used soft values for the short-range cutoff parameters in meson-baryon vertices (consistent with  $\pi N$  scattering) and obtained lower cross sections than other models which used larger cutoff

values fitted *ad hoc* to describe the magnitude of the  $pp \rightarrow d\pi^+$  cross section (see [54], Sec. III). Inclusion of dibaryon resonances is able to give the lacking short-range contributions to the cross sections and vector analyzing powers, however, without changing their qualitative behavior.

Quite the opposite situation takes place with the spin-correlation parameters, the results for which are shown in Fig. 7. It is well known that description of spin-correlation

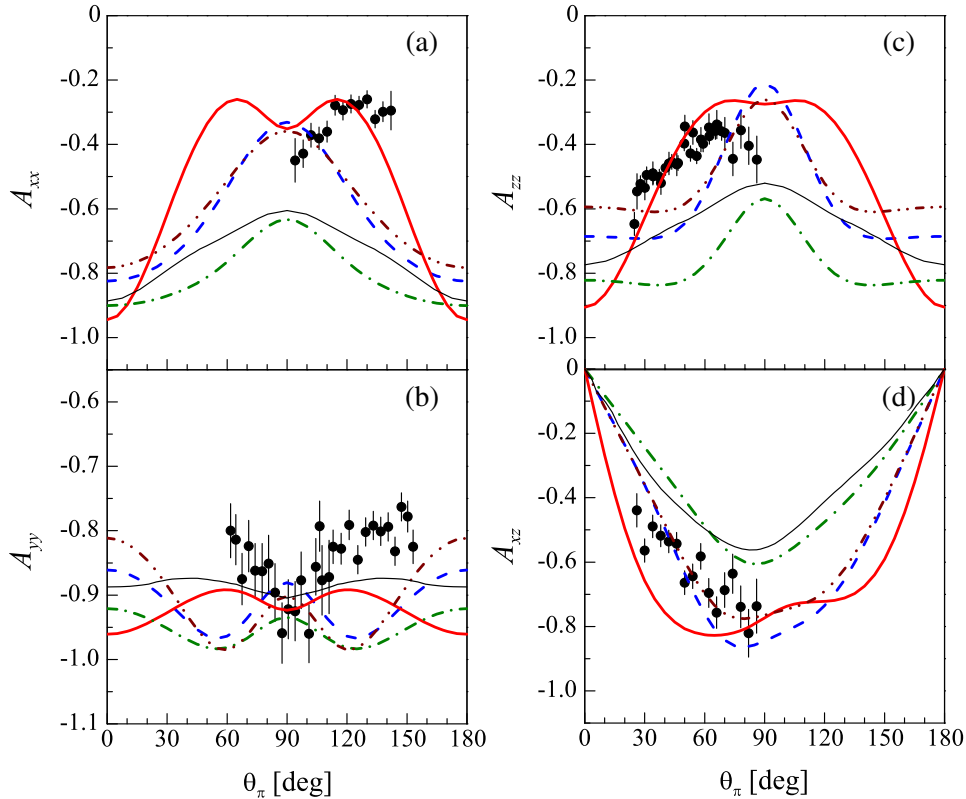


FIG. 7. Spin-correlation parameters (a)  $A_{xx}$ , (b)  $A_{yy}$ , (c)  $A_{zz}$ , and (d)  $A_{xz}$  in the reaction  $pp \rightarrow d\pi^+$  at energy  $T_p = 582$  MeV ( $\sqrt{s} = 2.15$  GeV). The meaning of theoretical curves is the same as in Fig. 5. Filled circles show the experimental data [77,78] for  $T_p = 578$  MeV.

parameters in the  $pp \rightarrow d\pi^+$  reaction was a serious problem for conventional theoretical models [54–56]. It was established long ago [56] that conventional meson-exchange mechanisms underestimate the contributions of triplet  $pp$  partial waves, which are very important for reproducing correctly the spin-correlation parameters. However, no definite solution for this problem has been found previously. As is seen from Fig. 7, just the  ${}^3P_2D$  amplitude and its interference with other amplitudes changes strongly the qualitative behavior of the spin-correlation parameters, thus giving them qualitative (or even semiquantitative) agreement with experimental data. And the proper magnitude of this amplitude can be obtained only by assuming a triplet  $P$ -wave dibaryon resonance excitation in addition to the conventional  $\Delta$  excitation [see Figs. 3(c) and 3(f)]. This is likely one of the most important results of the present study.

In view of this result, we can suggest the possible reason for improper behavior of spin-correlation parameters in the model calculations [48,49], which also included dibaryon resonances. Although the  ${}^3P_2$  resonance was included in these calculations, its parameters were not fitted individually, but together with parameters of the more intensive  ${}^1D_2$  and  ${}^3F_3$  resonances, to describe experimental data with mixed contributions of all resonances. As a result, its mass was found to be 2110 MeV and width 30 MeV, which are too low in comparison with experimental values and our results.

## V. DISCUSSION AND SUMMARY

In the paper, we studied the manifestation of isovector dibaryon resonances  ${}^1D_2$ ,  ${}^3F_3$  and  ${}^3P_2$  in the basic single-pion production reaction  $pp \rightarrow d\pi^+$ . All these resonances have been found in the PWA of  $pp$  elastic scattering [52,53]; however, the  $P$ -wave diproton resonance, being the least intensive, received less attention in the literature than the  $D$ - and  $F$ -wave resonances. A new experimental evidence of the  ${}^3P_2$  dibaryon has appeared just very recently [24] in the reaction  $pp \rightarrow (pp)_0\pi^0$  where the more intensive  ${}^1D_2$  and  ${}^3F_3$  resonances are forbidden by angular momentum and parity conservation.

We have found the large effects of the  ${}^3P_2$  diproton in the spin-correlation parameters of the  $pp \rightarrow d\pi^+$  reaction. In fact, the conventional models [54–56] (based mainly on the  $t$ -channel meson-exchange mechanisms) for this reaction generally resulted in underestimation and even improper behavior of the proton-proton spin-correlation parameters  $A_{xx}$ ,  $A_{yy}$  and  $A_{zz}$ . We should note here that the coupled-channel approach of Niskanen [55] appeared to be more successful than other conventional models for the  $pp \rightarrow d\pi^+$  reaction, while still giving essential underestimation of  $A_{xx}$  and  $A_{yy}$ . However this approach turned out to completely fail for a similar reaction  $pp \rightarrow (pp)_0\pi^0$ , as was discussed in detail in a recent experimental paper [24]. Thus, the most recent experimental data in this area are in strong

disagreement with the model predictions of Niskanen both in the forward cross section and in energy dependence. On the other hand, just these experimental data [24] revealed the existence of the  ${}^3P_2$  dibaryon. So, it is quite reasonable to suggest that the  ${}^3P_2$  dibaryon, which is clearly seen in the reaction  $pp \rightarrow (pp)_0\pi^0$ , should also manifest itself in a similar reaction  $pp \rightarrow d\pi^+$ , not in the unpolarized cross section where the dominant contributions are given by  ${}^1D_2$  and  ${}^3F_3$  dibaryons, however, but in more sensitive observables like spin-correlation parameters. In fact, we have shown that only assuming the contribution of the  $P$ -wave diproton resonance makes it possible to explain semiquantitatively the experimental data for these observables. By the way, this explanation is rather similar to the explanation of the proton polarization in the reaction  $d(\gamma, \vec{p})n$  at  $E_\gamma = 400$ – $600$  MeV found long ago in [80,81]. The strong disagreement for the outgoing proton polarization between the predictions of conventional models and experimental data [80] could only be explained by incorporation of the  ${}^3D_3$  and  ${}^3F_3$  intermediate dibaryon contributions. In this case one has another example of a process where the large spin-dependent observables could be explained only by assuming the intermediate dibaryon resonances.

Another interesting question worth discussing in connection with the  $P$ -wave diproton is the well-known puzzling behavior of the elastic  $NN$ -scattering phase shifts in the triplet  $P$  waves. In fact, while the triplet  ${}^3P_0$  and  ${}^3P_1$   $NN$  phase shifts (and also the singlet one  ${}^1P_1$ ) clearly demonstrate the short-range repulsive core behavior (with the core radius  $r_c \approx 0.9$  fm), the  ${}^3P_2$  phase shifts are rising up to 600 MeV (laboratory) and do not display any features of the repulsive core. However, in the conventional treatment of  $NN$  interaction, the short-range central-force repulsion should be a universal feature for all  ${}^3P_J$ ,  $J = 0, 1, 2$ . The puzzle has been resolved in the conventional One-Boson-Exchange (OBE) models [82] through introduction of a highly intensive short-range spin-orbit force which produces a very strong attraction just in the  ${}^3P_2$  channel and compensates completely the very large and broad repulsive core which is present in all  $P$  waves. This huge spin-orbit interaction looks rather unnatural and fitted *ad hoc* (for a detailed discussion of inconsistencies in the OBE-like  $NN$ -potential models see [83]).

The results of the present paper give some alternative explanation for the  $P$ -wave  $NN$  phase-shifts puzzle. In fact, one can think that the short-range  ${}^3P_2$  dibaryon with a mass  $M({}^3P_2) \approx 2.2$  GeV induces as usual a strong  $NN$  attraction [59], the strongest at laboratory energies  $T_N \approx 600$  MeV, so that the above dibaryon-induced attraction at intermediate energies can explain naturally the puzzling behavior of the  ${}^3P_2$   $NN$  phase shifts.

It is interesting to discuss further the possible quark structure of an isovector  $P$ -wave dibaryon and a mechanism of its decay with a pion emission. In the paper [47] we

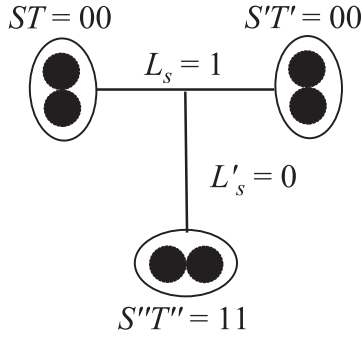


FIG. 8. Allowable three-diquark configuration for an isovector  $P$ -wave dibaryon.

adopted the two-cluster  $q^4 - q^2$  structure [84,85] for the series of isovector dibaryons  ${}^1D_2$ ,  ${}^3F_3$ ,  ${}^1G_4$ , etc., with a tetraquark  $q^4(S=1, T=0)$  and an axial diquark  $q^2(S'=T'=1)$  connected by a color QCD string with an orbital angular momentum  $L_s = 0, 1, 2$ , etc. The  ${}^3P_2$  isovector dibaryon apparently does not belong to this series. If we assume the two-cluster  $q^4 - q^2$  structure for this dibaryon as well, then the most appropriate structure would be a two-cluster state with a color string ( $L_s = 1$ ) connecting the tetraquark  $q^4(S=T=1)$  and a scalar diquark  $q^2(S'=T'=0)$ . However the tetraquark with  $S=T=1$  should be unstable against the decay into two (scalar and axial) diquarks. Then, the two scalar diquarks that result from such a decay into the three-diquark system must be in a mutual  $P$ -wave due to the Pauli exclusion principle (see Fig. 8).

The “natural” decay of the three-diquark state with a pion emission, viz.  $q^2(S''=T''=1) \rightarrow q^2(S''=T''=0)$  and  $L'_s = 0 \rightarrow L'_s = 1$ , is unlikely because the final state in this case would be the so-called “demon deuteron” [86] with two  $P$ -wave strings, which would have a higher mass than the initial  $P$ -wave dibaryon. Thus, the most probable transition should be the rearrangement of the three-cluster configuration shown in Fig. 8 to a conventional two-cluster  $q^3 - q^3$  state with a  $P$ -wave string between two  $3q$  clusters. Then this state, in its turn, decays via a single-pion emission to the final deuteron ( $S=1, T=0$ ) or singlet deuteron ( $S=0, T=1$ ), i.e., by the usual spin-flip or isospin-flip transitions.

A recent experiment [24] revealed the existence of the  ${}^3P_0$  dibaryon resonance, along with the  ${}^3P_2$  one. Besides that, the recent  $pp$ -scattering analysis [87] predicts three diproton resonances  ${}^3P_J, J=0, 1, 2$ . The decay of the  ${}^3P_0$  resonance into the  $d\pi^+$  channel is forbidden due to angular momentum and parity conservation, but it can decay into the  $(pp)_0\pi^0$  channel. For the same reasons, the  ${}^3P_1$  resonance can decay into  $d\pi^+$ , but not into the  $(pp)_0\pi^0$  channel. If the  ${}^3P_0$  and/or  ${}^3P_1$  dibaryons really exist, all of the above quark-structure considerations will hold for them too. However, these resonances obviously give a very small contribution to  $NN$  elastic scattering (compared to the background meson-exchange mechanisms), which is indicated by a very moderate attraction in the  ${}^3P_0$  channel and an almost negligible attraction in the  ${}^3P_1$  channel (compared to the strong attraction in the  ${}^3P_2$  channel—see the above discussion of the  $P$ -wave phase-shifts puzzle). Furthermore, these resonances, contrary to the  ${}^3P_2$  dibaryon, were not found in most phase-shift analyses of  $pp$  elastic scattering. So, further studies are needed to shed light on the existence and properties of the  $P$ -wave diproton resonances.

To summarize, we have shown that the intermediate dibaryon resonances in the  $NN$  channels  ${}^1D_2$ ,  ${}^3F_3$  and  ${}^3P_2$  are very likely to be responsible for a significant part of the cross sections of the basic single-pion production process  $pp \rightarrow d\pi^+$  in a broad energy range ( $T_p = 400\text{--}800$  MeV). Moreover, the  ${}^3P_2$  diproton resonance has been shown to be responsible for the most important characteristic features of the  $pp$  spin-correlation parameters in this reaction (at least near  $T_p \approx 600$  MeV). So, the role of the isovector dibaryons in single-pion production in  $pp$  collisions is rather similar to that of the isoscalar  ${}^3D_3$  dibaryon in double-pion production in  $pn$  collisions [20,88]. Besides that, the isovector dibaryons might play an important role also in double-pion production in  $pp$  collisions [47]. These results may have many far-reaching implications in hadronic and nuclear physics.

## ACKNOWLEDGMENTS

The work was done under partial financial support from Russian Foundation for Basic Research Grants No. 16-02-00049, No. 16-02-000265 and No. 16-52-12005. M. N. P. also appreciates support from the Dynasty Foundation.

- [1] R. L. Jaffe, *Phys. Rev. Lett.* **38**, 195 (1977).  
 [2] A. T. M. Aerts, P. J. G. Mulders, and J. J. de Swart, *Phys. Rev. D* **17**, 260 (1978).  
 [3] V. A. Matveev and P. Sorba, *Nuovo. Cim.* **45A**, 257 (1978).

- [4] I. P. Auer, A. Beretvas, E. Colton, D. Hill, K. Nield, H. Spinka, D. Underwood, Y. Watanabe, and A. Yokosawa, *Phys. Lett.* **70B**, 475 (1977).  
 [5] I. P. Auer *et al.*, *Phys. Rev. Lett.* **41**, 1436 (1978).  
 [6] E. K. Biegert *et al.*, *Phys. Lett.* **73B**, 235 (1978).

- [7] I. P. Auer *et al.*, *Phys. Rev. Lett.* **48**, 1150 (1982).
- [8] I. P. Auer *et al.*, *Phys. Rev. Lett.* **62**, 2649 (1989).
- [9] M. P. Locher, M. E. Sainio, and A. Svarc, *Adv. Nucl. Phys.* **17**, 47 (1986).
- [10] R. Bhandari, R. A. Arndt, L. D. Roper, and B. J. VerWest, *Phys. Rev. Lett.* **46**, 1111 (1981).
- [11] R. A. Arndt, L. D. Roper, R. L. Workman, and M. W. McNaughton, *Phys. Rev. D* **45**, 3995 (1992).
- [12] A. V. Kravtsov, M. G. Ryskin, and I. I. Strakovsky, *J. Phys. G* **9**, L187 (1983).
- [13] I. I. Strakovsky, A. V. Kravtsov, and M. G. Ryskin, *Sov. J. Nucl. Phys.* **40**, 273 (1984).
- [14] N. Hoshizaki, *Prog. Theor. Phys.* **60**, 1796 (1978).
- [15] N. Hoshizaki, *Prog. Theor. Phys.* **61**, 129 (1979).
- [16] Y. A. Simonov and M. van der Velde, *J. Phys. G* **5**, 493 (1979).
- [17] J. A. Niskanen, *Phys. Lett.* **112B**, 17 (1982).
- [18] I. I. Strakovsky, *AIP Conf. Proc.* **221**, 218 (1991).
- [19] A. Valcarce, H. Garcilazo, R. D. Mota, and F. Fernandez, *J. Phys. G* **27**, L1 (2001).
- [20] P. Adlarson *et al.* (WASA-at-COSY Collaboration), *Phys. Rev. Lett.* **106**, 242302 (2011).
- [21] P. Adlarson *et al.* (WASA-at-COSY Collaboration, SAID Data Analysis Center), *Phys. Rev. Lett.* **112**, 202301 (2014).
- [22] J. T. Goldman, K. Maltman, G. J. Stephenson, K. E. Schmidt, and F. Wang, *Phys. Rev. C* **39**, 1889 (1989).
- [23] F. J. Dyson and N.-H. Xuong, *Phys. Rev. Lett.* **13**, 815 (1964).
- [24] V. I. Komarov *et al.*, *Phys. Rev. C* **93**, 065206 (2016).
- [25] A. Gal and H. Garcilazo, *Phys. Rev. Lett.* **111**, 172301 (2013).
- [26] A. Gal and H. Garcilazo, *Nucl. Phys.* **A928**, 73 (2014).
- [27] M. Bashkanov, S. J. Brodsky, and H. Clement, *Phys. Lett. B* **727**, 438 (2013).
- [28] H. Huang, J. Ping, and F. Wang, *Phys. Rev. C* **89**, 034001 (2014).
- [29] Y. Dong, P. Shen, F. Huang, and Z. Zhang, *Phys. Rev. C* **91**, 064002 (2015).
- [30] S. J. Brodsky, C.-R. Ji, and G. P. Lepage, *Phys. Rev. Lett.* **51**, 83 (1983).
- [31] S. J. Brodsky and C.-R. Ji, *Phys. Rev. D* **33**, 1406 (1986).
- [32] CERN, *Courier* **54**, 6 (2014); <http://cerncourier.com/cws/article/cern/57836>.
- [33] A. I. Baz', *Adv. Phys. (Philos. Mag. Suppl.)* **8**, 349 (1959).
- [34] E. P. Wigner, *Phys. Rev.* **73**, 1002 (1948).
- [35] V. I. Serov and V. A. Zhmailo, *Sov. Phys. JETP* **17**, 227 (1963).
- [36] F. Ajenberg-Selove and T. Lauritsen, *Nucl. Phys.* **11**, 1 (1959).
- [37] C. Hanhart, Yu. S. Kalashnikova, and A. V. Nefediev, *Phys. Rev. D* **81**, 094028 (2010).
- [38] T. Hyodo, *Phys. Rev. Lett.* **111**, 132002 (2013).
- [39] R. A. Arndt, J. M. Ford, and L. D. Roper, *Phys. Rev. D* **32**, 1085 (1985).
- [40] K. A. Olive *et al.* (Particle Data Group), *Chin. Phys. C* **38**, 090001 (2014).
- [41] A. V. Sarantsev *et al.*, *Phys. Lett.* **659B**, 94 (2008).
- [42] T. Skorodko *et al.*, *Eur. Phys. J. A* **35**, 317 (2008).
- [43] I. T. Obukhovskiy, A. Faessler, D. K. Fedorov, T. Gutsche, and V. E. Lyubovitskij, *Phys. Rev. D* **84**, 014004 (2011).
- [44] A. Gal, *Acta Phys. Pol. B* **47**, 471 (2016).
- [45] R. Aaij *et al.* (LHCb Collaboration), *Phys. Rev. Lett.* **112**, 222002 (2014).
- [46] R. Aaij *et al.* (LHCb Collaboration), *Phys. Rev. Lett.* **115**, 072001 (2015).
- [47] M. N. Platonova and V. I. Kukulkin, *Nucl. Phys.* **A946**, 117 (2016).
- [48] H. Kamo and W. Watari, *Prog. Theor. Phys.* **62**, 1035 (1979).
- [49] H. Kamo and W. Watari, *Prog. Theor. Phys.* **64**, 338 (1980).
- [50] R. A. Arndt, I. I. Strakovsky, R. L. Workman, and D. V. Bugg, *Phys. Rev. C* **48**, 1926 (1993).
- [51] C.-H. Oh, R. A. Arndt, I. I. Strakovsky, and R. L. Workman, *Phys. Rev. C* **56**, 635 (1997).
- [52] R. A. Arndt, J. S. Hyslop III, and L. D. Roper, *Phys. Rev. D* **35**, 128 (1987).
- [53] Y. Higuchi, N. Hoshizaki, H. Masuda, and H. Nakao, *Prog. Theor. Phys.* **86**, 17 (1991).
- [54] G. H. Lamot, J. L. Perrot, C. Fayard, and T. Mizutani, *Phys. Rev. C* **35**, 239 (1987).
- [55] J. A. Niskanen, *Phys. Lett.* **141B**, 301 (1984).
- [56] W. Grein, A. König, P. Kroll, M. P. Locher, and A. Švarc, *Ann. Phys. (N.Y.)* **153**, 301 (1984).
- [57] M. Brack, D. O. Riska, and W. Weise, *Nucl. Phys.* **A287**, 425 (1977).
- [58] M. Jacob and G. C. Wick, *Ann. Phys. (N.Y.)* **7**, 404 (1959).
- [59] V. I. Kukulkin, I. T. Obukhovskiy, V. N. Pomerantsev, and A. Faessler, *J. Phys. G* **27**, 1851 (2001).
- [60] V. I. Kukulkin, I. T. Obukhovskiy, V. N. Pomerantsev, and A. Faessler, *Int. J. Mod. Phys. E* **11**, 1 (2002).
- [61] J. D. Jackson, *Nuovo Cimento* **34**, 1644 (1964).
- [62] V. V. Anisovich, E. M. Levin, A. K. Likhoded, and Y. G. Stroganov, *Sov. J. Nucl. Phys.* **8**, 339 (1969).
- [63] The SAID partial-wave analysis website, <http://gwdac.phys.gwu.edu/>.
- [64] O. Imambekov and Y. N. Uzikov, *Sov. J. Nucl. Phys.* **47**, 695 (1988).
- [65] K. F. Liu, S. J. Dong, T. Draper, D. Leinweber, J. Sloan, W. Wilcox, and R. M. Woloshyn, *Phys. Rev. D* **59**, 112001 (1999).
- [66] G. Erkol, M. Oka, and T. T. Takahashi, *Phys. Rev. D* **79**, 074509 (2009).
- [67] R. Machleidt, K. Holinde, and C. Elster, *Phys. Rep.* **149**, 1 (1987).
- [68] R. Machleidt, *Phys. Rev. C* **63**, 024001 (2001).
- [69] W. Koepf, L. L. Frankfurt, and M. Strikman, *Phys. Rev. D* **53**, 2586 (1996).
- [70] N. Hoshizaki, *Prog. Theor. Phys.* **89**, 251 (1993).
- [71] A. Yokosawa, *Int. J. Mod. Phys. A* **05**, 3089 (1990).
- [72] J. A. Niskanen and P. Wilhelm, *Phys. Lett. B* **359**, 295 (1995).
- [73] F. Shimizu, Y. Kubota, H. Koiso, F. Sai, S. Sakamoto, and S. S. Yamamoto, *Nucl. Phys.* **A386**, 571 (1982).
- [74] J. Hoftiezer, C. Weddingen, P. Chatelain, B. Favier, F. Foughi, C. Nussbaum, J. Piffaretti, S. Jaccard, and P. Walden, *Nucl. Phys.* **A402**, 429 (1983).
- [75] J. Hoftiezer, C. Weddigen, P. Chatelain, B. Favier, F. Foughi, J. Piffaretti, S. Jaccard, and P. Walden, *Nucl. Phys.* **A412**, 286 (1984).
- [76] G. R. Smith *et al.*, *Phys. Rev. C* **30**, 980 (1984).
- [77] E. Aprile *et al.*, *Nucl. Phys.* **A379**, 369 (1982).

- [78] E. Aprile *et al.*, *Nucl. Phys.* **A415**, 365 (1984).
- [79] T. Mizutani, C. Fayard, G. H. Lamot, and R. S. Nahabetian, *Phys. Lett.* **107B**, 177 (1981).
- [80] T. Kamae, I. Arai, T. Fujii, H. Ikeda, N. Kajiura, S. Kawabata, K. Nakamura, K. Ogawa, H. Takeda, and Y. Watase, *Phys. Rev. Lett.* **38**, 468 (1977).
- [81] T. Kamae and T. Fujita, *Phys. Rev. Lett.* **38**, 471 (1977).
- [82] A. Bohr and B. R. Mottelson, *Nuclear Structure* (World Scientific, Singapore, 1999), Vol. I.
- [83] V. I. Kukulín and M. N. Platonova, *Phys. At. Nucl.* **76**, 1465 (2013).
- [84] P. J. Mulders, A. T. M. Aerts, and J. J. De Swart, *Phys. Rev. D* **21**, 2653 (1980).
- [85] L. A. Kondratyuk, B. V. Martemyanov, and M. G. Shchepkin, *Sov. J. Nucl. Phys.* **45**, 776 (1987).
- [86] S. Fredriksson and M. Jändel, *Phys. Rev. Lett.* **48**, 14 (1982).
- [87] G. Papadimitriou and J. P. Vary, *Phys. Lett. B* **746**, 121 (2015).
- [88] M. N. Platonova and V. I. Kukulín, *Phys. Rev. C* **87**, 025202 (2013).